American Mineralogist, Volume 68, pages 1160–1168, 1983

A TEM study of the biotite–chlorite reaction and comparison with petrologic observations

DAVID R. VEBLEN

Department of Earth and Planetary Sciences
The Johns Hopkins University
Baltimore, Maryland 21218

AND JOHN M. FERRY

Department of Geology
Arizona State University
Tempe, Arizona 85281

Abstract

A biotite that has substantially altered to chlorite in a granitic rock from south-central Maine has been investigated with high-resolution and analytical transmission electron microscopy. The reaction takes place primarily by the replacement of TOT mica layers in the biotite by brucite-like layers (mechanism 2). This mechanism is different from that observed in other studies, in which the brucite-like layers grow into the interlayer planes of mica (mechanism 1). The reaction in the present case is accompanied by the formation of micro-precipitates, possibly of quartz or amorphous silica, on the planes of alteration. These precipitates, which can be as small at 20Å in largest dimension, deform the layers of the sheet silicates and apparently dissolve after complete conversion to chlorite has occurred.

The chemical and physical consequences of the two reaction mechanisms noted above can be predicted and are quite different. The changes in chemistry and sheet silicate volume expected from the observed mechanism (2) match very closely the changes inferred by Ferry (1979) on the basis of textural and chemical arguments. The agreement between chemical and volume changes predicted by mechanism 1 and Ferry's data are poor. The microscopic crystallographic and larger-scale petrologic observations are thus consistent with each other.

Introduction

Solid-state reactions that transform one sheet silicate into another occur commonly in nature. Important examples are provided by the progressive metamorphism of pelitic rocks, in which sedimentary sheet silicates are transformed sequentially into metamorphic sheet silicates of increasing grade (see, for example, Frey, 1969, 1978). Such reactions can also occur during retrograde metamorphism or the metamorphism of igneous rocks, as in the common reaction of biotite to chlorite.

Until recently, the transformation processes in sheet silicates were studied either by petrographic and chemical methods or by powder X-ray diffraction techniques. While these traditional methods are useful for recognizing rocks in which reaction has taken place and for identifying the reactant and product phases, generally they are not suitable for pinpointing the precise structural mechanisms of reaction. On the other hand, several recent transmission electron microscopy (TEM) studies have demonstrated the utility of this method for studying the mechanisms of these solid-state reactions in sheet silicates. For example, brucite-like layers intercalated in biotite (Iijima and Zhu, 1983; Olives Baños *et al.*, 1983), in talc (Veblen and Buseck, 1980, 1981; Veblen, 1980) and in the sodium trioctahedral mica wonesite (Veblen, 1983a,b) have been resolved with high-resolution (HRTEM) techniques. It is likely that at least some of these brucite-like layers, which produce local chlorite structural configurations in the micas, are the result of post-crystallization reactions (Iijima and Zhu, 1982; Olives Baños *et al.*, 1983). However likely this interpretation seems, in the specimens that have been studied with TEM methods, the microstructures are not suitable for rigorously distinguishing between an origin by solid-state reaction rather than by primary growth (Veblen, 1983b).

0003–004X/83/1112–1160$02.00

In the present study, a partially chloritized biotite from a granitic rock was examined with HRTEM and analytical TEM methods. Because this plutonic mica clearly crystallized as biotite, its microstructures definitely are the result of post-crystallization reaction, rather than primary growth processes. It is therefore possible to use the following observations to explore the mechanisms and chemical processes involved in the reaction of biotite to chlorite. In a rare convergence of techniques, the results of this TEM study can be related directly to the chemical consequences deduced from the earlier petrographic and electron microprobe investigations of Ferry (1979)!

Specimen description, experimental techniques, and image interpretation

The specimen employed in this study is number 1 from locality 698 of Ferry (1978, 1979) and has been thoroughly described in those papers. In brief, the biotite occurs in a muscovite–biotite–garnet quartz monzonite of Devonian age that was hydrothermally altered at approximately 425°C, 3500 bars, by a water-rich fluid (X_{CO_2} = 0–0.13). The quartz monzonite, which intruded the Waterville and Vassalboro Formations in south-central Maine, is apparently synmetamorphic, but it postdates all or almost all of the penetrative deformation in the area. The biotite has altered partially on a scale easily observable in thin section (Fig. 1), to chlorite and titanite (sphene); the titanite was not observed in this TEM study, possibly as a result of selective removal of this mineral during sample preparation, or because all of the titanite occurs as relatively large crystals, rather than as submicroscopic inclusions hidden in the sheet silicates. The trioctahedral mica is an iron-rich titaniferous biotite, and the chlorite is a ripidolite; chemical compositions derived by microprobe analysis are listed by Ferry (1979).[1] Electron diffraction patterns (this study) indicate that the primary biotite occurs in 1-layer, 2-layer, and disordered polytypic forms, with varying amounts of disorder in the 1-layer and 2-layer variations.

Specimens were prepared by argon ion milling of fragments of petrographic thin section; they were lightly coated with carbon. Electron microscopy was performed at 100 kV in a Philips 400T microscope, and qualitative analyses were obtained with a Tracor Northern TN2000 X-ray analyser, as described in more detail by Veblen (1983a). Image interpretation for the biotite and chlorite follows that of Veblen (1983b) and is consistent with observations by Iijima and Buseck (1978), Amouric *et al.* (1981), Iijima and Zhu (1982), Olives Baños *et al.* (1983), and Veblen and Buseck (1979, 1980, 1981) and with calculations by Spinnler, Self, Iijima, and Buseck (Gerard E. Spinnler, pers. comm., 1983). As in these papers, multiple-beam bright-field microscopy was conducted under conditions in which the structural layers of the sheet silicates are imaged as dark fringes, and interlayer regions appear as white fringes. Unfortunately, at the time of this TEM study, the microscope objective lens current was unstable, so that the resolution in many of the micrographs was degraded, and the brucite-like sheets were not fully resolved; it was still possible, however, to recognize the positions of the brucite-like sheets under these conditions by noting anomalous spacings between the TOT (tetrahedral–octahedral–tetrahedral) mica layers and by noting that where the brucite-like layers were not resolved they produced contrast that is lighter than that formed by the mica structure.

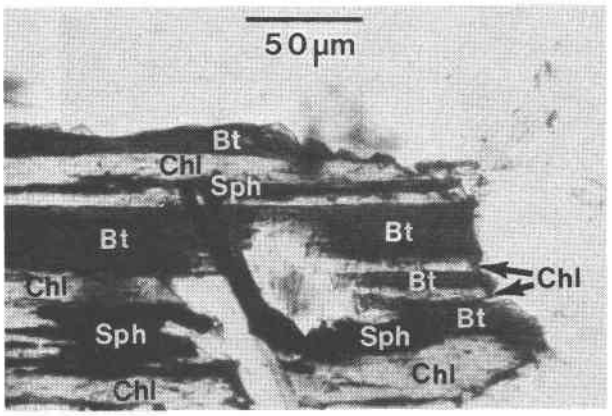

Fig. 1. Photomicrograph in plane polarized light of an intergrowth of biotite (Bt), chlorite (Chl), and titanite (Sph) from this study. The intergrowth is surrounded by quartz, microcline, and muscovite. The biotite and chlorite are intergrown on (001).

Mixed layering and other features in biotite and chlorite

Brucite-like layers in biotite

The intercalation of brucite-like layers is common throughout the biotite of this specimen, producing local chlorite structural configurations, as discussed previously (Veblen and Buseck, 1979, 1980, 1981; Veblen, 1980, 1983b; Iijima and Zhu, 1982; Olives Baños *et al.*, 1983; Cressey *et al.*, 1982). While some regions of biotite are completely free of these intercalation defects, most of the biotite contains them.

Of critical importance for the determination of structural mechanisms of reaction are the terminations of these brucite-like (or chlorite-like) layers in the biotite. Figure 2a shows one possible configuration, in which the brucite-like layer terminates in the interlayer region of the biotite; this microstructure could result from either primary growth or from a solid-state reaction in which the brucite-like layer replaces the interlayer region of the mica,

[1] Formulae from Ferry (1979):
Biotite—$K_{0.95}Na_{0.01}Mg_{0.59}Fe^{2+}_{1.65}Mn_{0.04}Ti_{0.18}Al_{1.63}Si_{2.72}O_{10}(OH)_2$
Chlorite—$Mg_{1.18}Fe^{2+}_{3.11}Mn_{0.09}Al_{2.80}Si_{2.71}O_{10}(OH)_8$

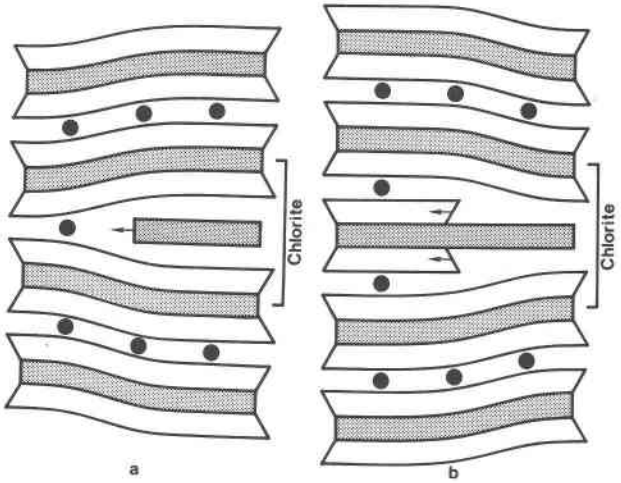

Fig. 2. Schematic representations of two different mechanisms for forming a single layer of chlorite in biotite. The degree of distortion of the TOT layers is exaggerated, because relaxation around terminated layers really occurs over a greater distance than that shown. Circles indicate interlayer cations. a. Mechanism 1. Growth of a brucite-like layer into the interlayer region between two TOT mica layers. Direction of growth of the layer is indicated by the arrow. This mechanism requires introduction of substantial material and results in an increase in volume. b. Mechanism 2. Formation of a brucite-like layer by removal of the tetrahedral sheets of one TOT mica layer. Direction of dissolution of the tetrahedral sheets is indicated by the arrows. This mechanism requires a net removal of material from the crystal and results in a decrease in volume.

forcing the mica layers apart and causing a volume increase. Terminations of this sort have been observed in talc (Veblen and Buseck, 1980, 1981; Veblen 1980), in biotite (Olives Baños *et al.*, 1983), and in the sodium trioctahedral mica wonesite (Veblen, 1983b). An alternative type of termination is shown in Figure 2b. In this case, both a brucite-like layer and a TOT talc-like (or mica) layer terminate, one becoming the other. This microstructure could again result from primary growth, or it could form by a reaction in which the brucite-like layer replaces the mica layer by removal of the mica tetrahedral sheets, causing a volume decrease; terminations of this sort have not been reported previously.

Figure 3 shows an experimental image from the present study of the mutual termination of brucite-like and mica layers. Since it is clear that the mica layer terminates, the structure is that of Figure 2b, rather than 2a. Inspection of the termination also shows that growth of the chlorite layer would entail a volume decrease, as in Figure 2b. A number of terminations of this sort were observed, while the other type is apparently absent. Because the brucite-like layers in this specimen are definitely the result of solid-state reaction, it can be concluded that the brucite-like layers observed in the biotite formed by consumption of mica layers. The petrological relevance of this observation is assessed in the "Discussion" section.

It has been recognized in other studies (*e.g.*, Olives Baños *et al.*, 1983; Bell and Wilson, 1981) that slip planes resulting from natural deformation can play an important role in the chemical behavior of micas. For example, basal slip planes can provide preferred sites for alteration reactions. In the present study, however, deformation of the biotite should not be an important factor, because crystallization and subsequent alteration of the specimen postdated all or almost all of the Devonian penetrative deformation in south-central Maine. Furthermore, evidence of deformation was absent from the mica, and, as shown above, alteration proceeded not along interlayer planes, where slip occurs, but along the TOT mica layers.

Micro-precipitates

One unusual observation in this specimen was the occurrence of small lenticular or plate-like precipitates in the planes of the brucite-like layers intercalated in biotite. These objects ranged in size from about 10Å to 120Å normal to the sheet silicate layers and from about 20Å to 600Å parallel to the layers. Two examples of these micro-precipitates are shown in Figure 4. It can be seen clearly that they deform the surrounding sheet silicate structure. Because literally thousands of these precipitates were

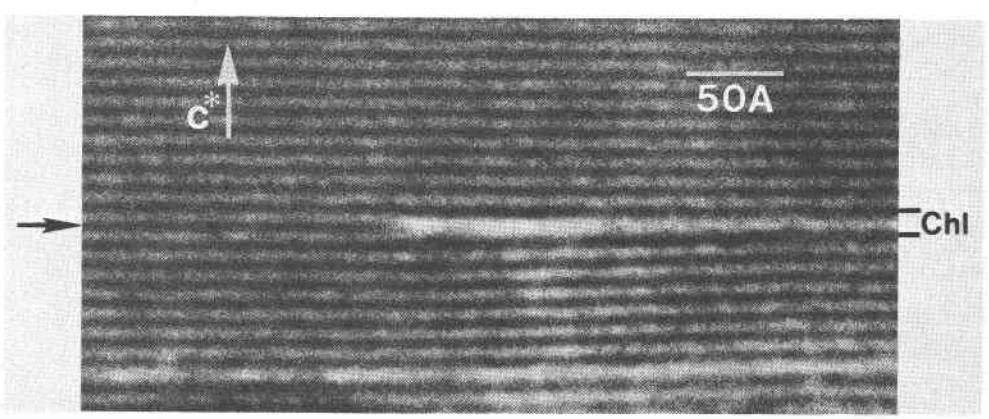

Fig. 3. Termination of a mica layer (arrowed) into a chlorite layer (Chl).

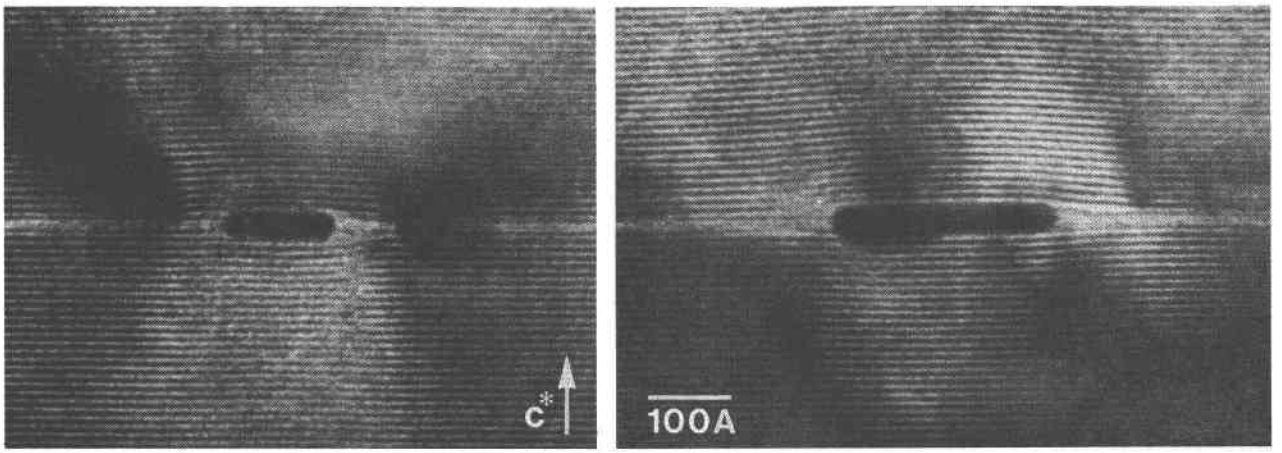

Fig. 4. Two examples of microprecipitates lying in planes where biotite has been altered to chlorite. These two examples are typical of the size range of most of the precipitates. Deformation of the mica layers around the precipitates can be seen best by viewing the figure at a low angle parallel to the layers.

observed, they should be treated as an important observation, rather than a curiosity.

These micro-precipitates exhibit no fringes in HRTEM and produce no recognized effects in selected area electron diffraction (SAED) patterns, suggesting that they may be amorphous. Failure to observe these effects, however, could result from their relatively small volume (compared to biotite), their non-rational orientation with respect to the electron beam, and spacings below the resolution of the TEM used in this study. In a few cases, moiré patterns were observed to be associated with the precipitates (Fig. 5). These could arise from interaction of a crystalline precipitate and the biotite. However, they could also be produced by overlapping of biotite above and below the precipitate, if the precipitate is completely embedded in the specimen and if it causes misorientation of the biotite above and below it. The question of whether the micro-precipitates are amorphous or crystalline is therefore not resolved by this study.

Attempts to analyze these micro-precipitates in the TEM were unsuccessful because of their small sizes. They were therefore not identified directly, although they may well be amorphous silica or quartz, based on petrological inference (see "Discussion"). Analysis using electron energy loss spectroscopy (EELS) and microdiffraction techniques on a dedicated scanning TEM (STEM) might provide a definitive identification.

Although the micro-precipitates were not identified rigorously, they clearly are an important and integral part of the alteration reaction in this biotite. In all cases, they lie in the planes of alteration, where a brucite-like layer has replaced a mica layer. In areas that have experienced substantial alteration, the micro-precipitates are abundant (Fig. 6), and they are also present in chlorite that is in the immediate proximity of partially-altered material. However, they appear to be absent in chlorite that is farther from biotite and from partially altered material; the significance of this observation is addressed in the "Discussion."

Substantially altered areas

As shown above, most regions of biotite that have undergone substantial alteration contain numerous micro-precipitates between the sheet silicate layers (Figs. 4, 6). They also, of course, contain numerous brucite-like layers, leading to both isolated and clumped areas of chlorite structure. This material can be described as an apparently random biotite–chlorite mixed-layer silicate (Fig. 7). This mixed-layer material is analogous to the wonesite–chlorite mixed-layer silicate described by Veblen (1983b),

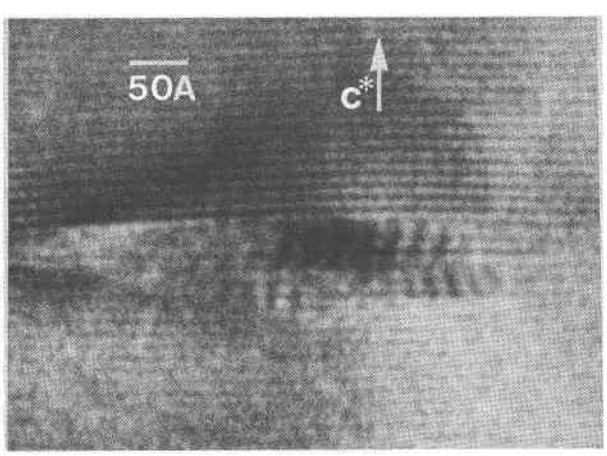

Fig. 5. Moiré fringes (diffuse, roughly vertical bands) associated with a micro-precipitate. Deformation of the mica around the precipitate can be seen by viewing at a low angle parallel to the mica layers.

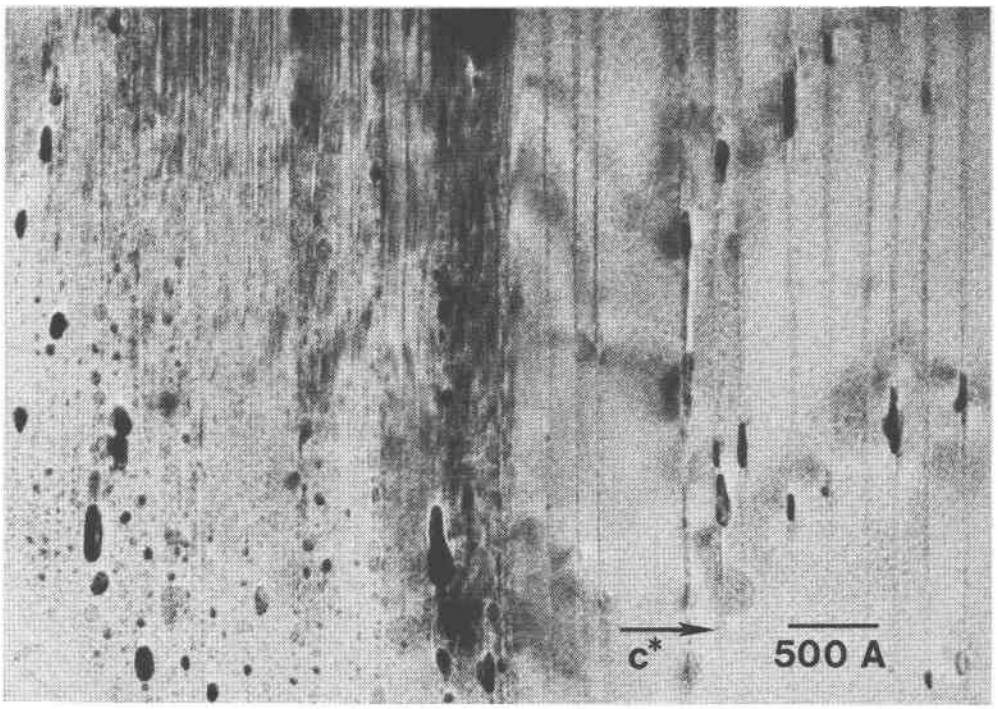

Fig. 6. Overview showing abundant precipitates (oblong black features). On the right, the precipitates lie on individual chlorite layers (vertical streaks) in biotite. On the left, the biotite has been more completely altered to a biotite–chlorite mixture.

except that the trioctahedral mica wonesite is sodium-rich instead of an ordinary potassium biotite.

Continued alteration of the biotite–chlorite intergrowth resulted in chlorite, which in some places contains a substantial number of relict extra mica layers and in other places is relatively free of these "defects." Rather than being a "perfect" chlorite that produces electron diffraction patterns and images characteristic of well-crystallized minerals, much of the chlorite appears to be highly defective. Images of much of this chlorite suggest that some layers of the structure are only poorly crystalline (Fig. 8).

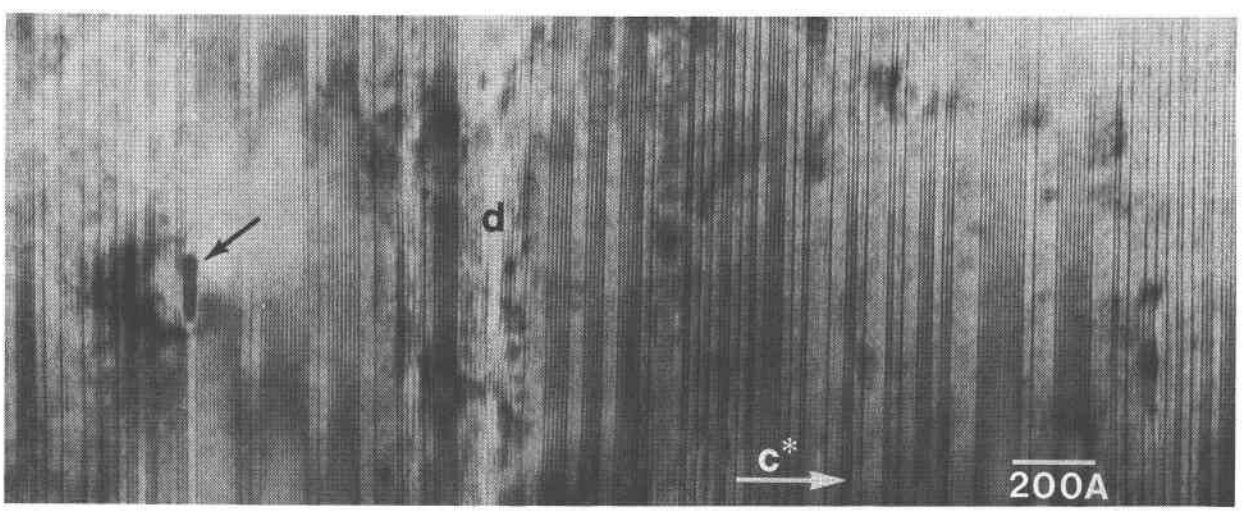

Fig. 7. Disordered mixed-layer biotite–chlorite. The mica has darker contrast with pronounced 10Å fringes, while the chlorite is lighter grey with lower contrast. The black arrow indicates a prominent micro-precipitate, and "d" indicates a disrupted region where the specimen has started to pull apart, presumably during sample handling.

Chemical characteristics

Energy-dispersive X-ray analyses obtained in the TEM from the biotite and chlorite confirm the electron microprobe results of Ferry (1979): the most notable differences are that the biotite contains substantial K and Ti, while the chlorite does not, and the chlorite contains substantially less Si than the biotite (these are not surprising results!). The relative proportions of Mg, Fe, and Al are not much affected by the alteration of the sheet silicate from biotite to chlorite.

Analyses of the mixed-layer materials show that these are intermediate in chemical composition between biotite and chlorite. Although the analyses are not quantitative, they are at least consistent with the notion that there is a linear relationship between degree of structural reaction and the chemical composition. Such a relationship has been demonstrated for partially-reacted chain silicate systems (Veblen, 1981) and stems from the fact that individual structural elements in an intergrowth exhibit essentially the same cation partitioning behavior that they would in their pure end-member structures. This property, in turn, results from the fact that partitioning behavior of crystallographic sites is largely determined by nearest-neighbor site geometry, rather than by more distant parts of the structure. Thus, the brucite-like layers in the mixed-layer materials behave chemically just as they do in the pure chlorite, for example.

Discussion

It has been shown above that in this specimen of biotite from a granitic rock, alteration to chlorite proceeded by a mechanism in which brucite-like layers replaced TOT mica layers. We now examine the chemical consequences of different reaction mechanisms and relate them to the chemical characteristics of the alteration process as derived from the electron microprobe and petrographic study of Ferry (1979). If one knows the precise structural mechanism of reaction, it is possible to predict certain bulk chemical and physical attributes of the reaction. For example, the complete replacement of a biotite crystal by the mechanism shown in Figure 2a (mechanism 1) would require the interjection of brucite-like layers into the interlayer regions between all TOT talc-like layers in the structure, along with removal of the interlayer cations. For the molar volumes in this particular occurrence (Ferry, 1979), this would entail a volume increase of 39.8%. This mechanism would also require the introduction of considerable amounts of Fe, Mg, Al, and H, which are necessary for the construction of the brucite-like layers. Additionally, K would diffuse out of the structure along the terminations of the brucite-like layers, and Ti would be required to diffuse out of the octahedral sites of the TOT mica layers, being replaced by Fe, Mg, and Al.

The reaction mechanism depicted in Figure 2b (mechanism 2) produces much different chemical and physical results from that of Figure 2a (mechanism 1). Because the brucite-like layer replaces a larger TOT layer, this mechanism results in a volume reduction. For complete reaction to chlorite, one-half of the TOT layers would be replaced by brucite-like layers, giving a volume loss of 30.1% for the biotite and chlorite compositions of this occurrence. The overriding chemical consequences of this mechanism are the removal of Si and alkalis and the addition of H, with relatively minor removal of Fe and Al to compensate for loss of the tetrahedrally-coordinated Al sites. Removal of Ti would require addition of Fe, Mg, or Al to the octahedral sites of the TOT layer, but this effect is smaller than that of the lost tetrahedral sites on the budget for Fe, Mg, and Al.

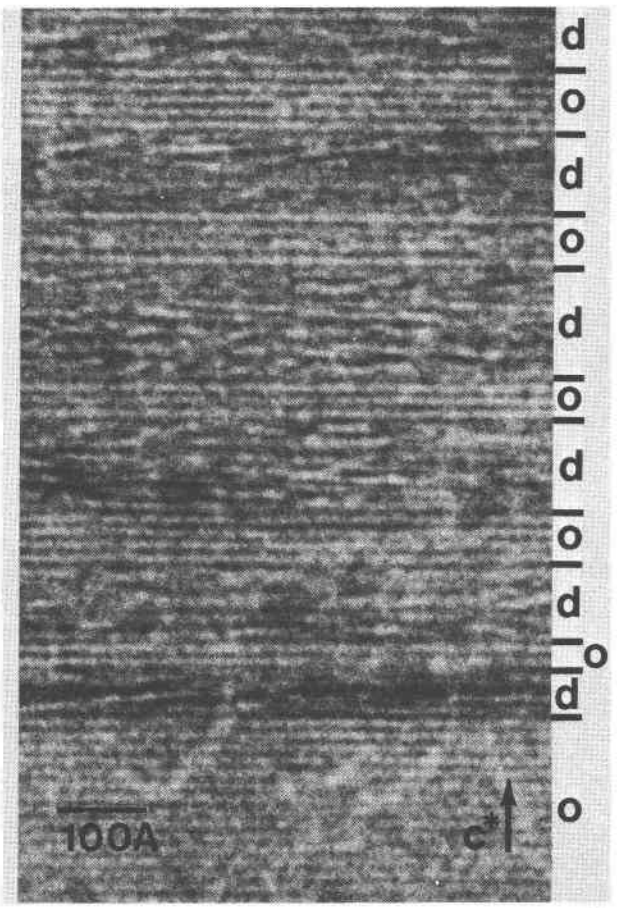

Fig. 8. Interlayering of relatively ordered chlorite (o), with periodic 14Å fringes, and disordered material (d). Although some semblance of a layer structure can be discerned in the disordered regions, the layers appear to be discontinuous and not perfectly straight.

Based on petrographic interpretations and electron microprobe data, Ferry (1979) used a constant Al and Ti reference frame to assess the likely chemical processes and change in volume for the reaction of biotite to chlorite plus titanite in this rock. Subtracting out from Ferry's results the chemical effects of the titanite, which has not

been considered in the above structural discussion of reaction mechanisms, we arrive at the following chemical changes necessary for the transformation of the biotite to chlorite at constant Al: large introductions of H_2O and H^+; relatively minor introductions of Mg and Fe; and major losses of K and Si (presumed to be in the form of H_2SiO_4). Again subtracting out the contribution of titanite, the volume change predicted by Ferry's results would be a decrease of 18.6%. (See Appendix I for a description of how the effects of titanite were subtracted from the reaction of Ferry, 1979.)

Some of these results, normalized to 1.00 formula units of biotite, are summarized in Table 1. The numbers in this table refer to the reaction coefficients for chlorite; Fe + Mg + Mn; Al; H_4SiO_4; H^+; and H_2O that would result from reaction mechanisms 1 and 2 and from the mass balance calculations of Ferry (1979), adjusted as described above. Coefficients for the products are taken as positive, those of reactants negative. Also included in Table 1 are the volume changes deduced from reaction mechanisms and those of Ferry. The mineral compositions of Ferry were used for the two reaction mechanism calculations, combined with the assumptions (1) that Ti in biotite is removed in the form of Ti^{4+}; (2) as in Ferry (1979), Si is removed in the form of H_4SiO_4, K in the form of K^+, *etc.* No assumption was made concerning the mobility or immobility of any of the chemical species (*i.e.*, there was no assumption of a constant Al reference frame). (See Appendix I for the detailed forms of these reactions.)

Table 1 shows that there is relatively good agreement between the calculations of Ferry (1979) and the effects of reaction mechanism 2, which is the mechanism that is actually observed to occur in this case. It is gratifying indeed that we can relate the microscopic mechanisms of a reaction to the macroscopically observable textures and chemistry that result from it.

There are several possible explanations for the rather minor discrepancies between mechanism 2 and Ferry's calculations. First, it is possible that more than one reaction mechanism operated; note that if approximately 85% of the biotite reacted to chlorite via mechanism 2, while only 15% reacted via mechanism 1, the agreement with Ferry's calculations would be superb. It is very possible, given the relatively small number of terminations of brucite-like layers that are present in the specimen, that small numbers of terminations from mechanism 1 would not have been observed, even if they had been present. Alternatively, it is possible that after substantial reaction has taken place via mechanism 2, another mechanism takes over. Given the textures that were observed in this TEM study, it would be difficult to recognize whether a bulk reaction mechanism, for example, had operated during the final stages of reaction or not.

Table 1. Selected reaction coefficients and volume changes calculated from reaction mechanisms, compared with those estimated by Ferry (1979).

Coefficient in the Reaction	Mechanism 1	Mechanism 2	Ferry (1979)
Chlorite	+1.00	+0.50	+0.58
Fe + Mg + Mn	-2.10	+0.32	-0.37
Al	-1.17	+0.23	0.00
H_4SiO_4	+0.01	+1.36	+1.14
H^+	+6.03	-2.55	-0.06
H_2O	-6.04	-2.45	-3.23
$\Delta V/\bar{V}^\circ_{Bi}$	+39.8%	-30.1%	-18.6%

Another possible explanation for the minor discrepancy between mechanism 2 and the calculations of Ferry (1979) is that Ferry's assumptions of constant Al (and Ti) are not rigorously correct. Although it appears to be true that Al is relatively immobile in the metamorphic environment, it is possible that some Al was transported in the case of this reaction; allowing only a small amount of Al to migrate out of the sheet silicate would bring the two results into virtually complete agreement. In any case, the agreement between observed reaction mechanism 2 and the chemical details of the reaction as deduced from petrological observations is quite good, while agreement between mechanism 1, which has apparently been observed in other occurrences (see above), and the petrological deductions is very bad.

Another chemical aspect of this reaction involves the role of H^+ ions. As discussed by Carmichael (1969), short-range electrostatic neutrality can require transport of H_2O and H^+ to and from reaction sites. In the present case, the two reaction mechanisms require very different behavior of H. As shown in Table 1, mechanism 1 should produce large numbers of H^+ ions to compensate for the influx of Fe, Mg, and Al ions, while mechanism 2 would require an influx of H^+. Mechanism 1 can thus be expected to be favored in an environment of low H^+ activity, while mechanism 2 would be favored in an acidic environment. It also should be noted that other alteration reactions occurring in this rock apparently produced H^+, so that a local source for the H^+ required for mechanism 2 presumably existed during the alteration (Ferry, 1979).

One question left unanswered by this study concerns the identity of the micro-precipitates that are observed to form along the planes of reaction. Although no direct analysis of these precipitates was possible, it seems likely that they contain an element or elements from the biotite that are "rejected" by the chlorite. Since the reaction produces macroscopically-observable titanite, it might at first seem that the micro-precipitates are also titanite, but on a finer scale. However, regions of chlorite in which these precipitates are abundant show no Ti in X-ray analyses performed in the TEM, so that this is not the case. Other likely possibilities involve the tetrahedral cations Si and Al. Since the ratio Al/(Fe + Mg + Al) does not change much, and since a large amount of Si is

released by the reaction, the most likely explanation of these micro-precipitates is that they are extremely fine inclusions of quartz or amorphous silica.

The micro-precipitates occur along isolated planes that have reacted to brucite-like layers and are abundant in partially reacted material (Fig. 6) and in chlorite that is close to such material. They are, however, absent from much of the completely reacted chlorite. It thus seems that they form during the reaction as a result of insufficient transport out of the crystal of components produced by the reaction. In the end, however, given enough time, they dissolve. It may be in part this process of precipitation followed by dissolution that leaves much of the final chlorite structurally deranged.

In closing, let us note that solid-state reactions are commonly characterized by petrologists in terms of macroscopically observable parameters and by crystallographers in terms of microscopic crystal-structural parameters. However, these alternative descriptions, albeit of different scales, are related. We need not ask whether the chemical changes in minerals control the crystallographic changes, or *vice versa*. To more fully understand both the crystallography and the petrology, we should, however, consider both the microscopic mechanisms of reaction and the more readily observable textural and chemical changes.

Acknowledgments

We thank Drs. Dugald M. Carmichael, David A. Hewitt, Adrian J. Brearley, and James N. Boland for constructive reviews. This work was supported by NSF grants EAR81-15790 and EAR83-06861 to DRV and EAR80-20567 to JMF. Electron microscopy was performed in the Facility for HREM, Arizona State University, which was established with partial support from NSF grant CHE79-16098.

References

Amouric, Marc, Mercuriot, G., and Baronnet, Alain (1981) On computed and observed HRTEM images of perfect mica polytypes. Bulletin de Minéralogie, 104, 298–313.

Bell, I. A. and C. J. L. Wilson (1981) Deformation of biotite and muscovite: TEM microstructure and deformation model. Tectonophysics, 78, 201–228.

Carmichael, D. M. (1969) On the mechanism of prograde metamorphic reactions in quartz-bearing pelitic rocks. Contributions to Mineralogy and Petrology, 20, 244–267.

Cressey, B. A., Whittaker, E. J. W., and Hutchison, J. L. (1982) Morphology and alteration of asbestiform grunerite and anthophyllite. Mineralogical Magazine, 46, 77–87.

Ferry, J. M. (1978) Fluid interaction between granite and sediment during metamorphism, south-central Maine. American Journal of Science, 278, 1025–1056.

Ferry, J. M. (1979) Reaction mechanisms, physical conditions, and mass transfer during hydrothermal alteration of mica and feldspar in granitic rocks from south-central Maine, USA. Contributions to Mineralogy and Petrology, 68, 125–139.

Frey, Martin (1969) A mixed-layer paragonite/phengite of low-grade metamorphic origin. Contributions to Mineralogy and Petrology, 24, 63–65.

Frey, Martin (1978) Progressive low-grade metamorphism of a black shale formation, central Swiss Alps, with special reference to pyrophyllite and margarite bearing assemblages. Journal of Petrology, 19, 95–135.

Iijima, Sumio and Buseck, P. R. (1978) Experimental study of disordered mica structures by high-resolution electron microscopy. Acta Crystallographica, A34, 709–719.

Iijima, Sumio and Zhu, Jing (1982) Electron microscopy of a muscovite-biotite interface. American Mineralogist, 67, 1195–1205.

Olives Baños, Juan, Amouric, Marc, de Fouquet, Chantal, and Baronnet, Alain (1983) Interlayering and interlayer slip in biotite as seen by HRTEM. American Mineralogist, 68, 754–758.

Veblen, D. R. (1980) Anthophyllite asbestos: microstructures, intergrown sheet silicates, and mechanisms of fiber formation. American Mineralogist, 65, 1075–1086.

Veblen, D. R. (1981) Non-classical pyriboles and polysomatic reactions in biopyriboles. In D. R. Veblen, Ed., Amphiboles and Other Hydrous Pyriboles—Mineralogy, Mineralogical Society of America Reviews in Mineralogy, 9A, p. 189–236. Washington, D.C.

Veblen, D. R. (1983a) Exsolution and crystal chemistry of the sodium mica wonesite. American Mineralogist, 68, 554–565.

Veblen, D. R. (1983b) Microstructures and mixed layering in intergrown wonesite, chlorite, talc, kaolinite, and biotite. American Mineralogist, 68, 566–580.

Veblen, D. R. and Buseck, P. R. (1979) Serpentine minerals: intergrowths and new combination structures. Science, 206, 1398–1400.

Veblen, D. R. and Buseck, P. R. (1980) Microstructures and reaction mechanisms in biopyriboles. American Mineralogist, 65, 599–623.

Veblen, D. R. and Buseck, P. R. (1981) Hydrous pyriboles and sheet silicates in pyroxenes and uralites: intergrowth microstructures and reaction mechanisms. American Mineralogist, 66, 1107–1134.

Manuscript received, August 30, 1982;
accepted for publication, May 3, 1983.

Appendix I: Reaction recalculation methods

The reaction given by Ferry (1979), normalized to 1 mole of biotite, is as follows:

$$1\ \mathrm{Bi} + 3.23\mathrm{H_2O} + 0.06\mathrm{H^+} + 0.10\mathrm{Mg^{2+}} + 0.16\mathrm{Fe^{2+}} + 0.01\mathrm{Mn^{2+}}\ 0.18\mathrm{Ca^{2+}} = 0.58\mathrm{Chl} + 0.18\mathrm{Titanite} + 0.96\mathrm{H_4SiO_4} + 0.96\mathrm{K^+} + 0.01\mathrm{Na^+}$$

The molar volumes calculated by Ferry are $\bar{V}^0_{\mathrm{Bi}} = 152.21\mathrm{cm}^3$ for the biotite and $\bar{V}^0_{\mathrm{Chl}} = 212.85\mathrm{cm}^3$ for the chlorite.

For the purposes of the present study, the effects of the titanite in the above reaction were removed, in order to compare the volume change and chemical effects of the biotite to chlorite transformation with those derived from reaction mechanisms. This procedure is justified by the observation that on the microscopic scale Ti is removed from the biotite and not reincorporated into chlorite. Instead, it migrates some distance to form relatively large titanite crystals (see Fig. 1), and the reaction observed on the TEM scale is biotite to chlorite.

The volume change for the biotite to chlorite reaction was calculated simply as

$$-\Delta V/\bar{V}^0_{Bi} = \frac{\bar{V}^0_{Bi} - 0.582\bar{V}^0_{Chl}}{\bar{V}^0_{Bi}}.$$

The chemical effects of the titanite were subtracted from the above reaction by assuming it to be stoichiometric $CaTiSiO_5$, in accord with analytical results of Ferry (1979). Thus, the 0.18 moles of Ca^{2+} necesasry to make 0.18 moles of titanite were subtracted from the reactants; 0.18 moles each of Si and Ti in the titanite were added to the products; H_2O and H^+ were also adjusted to balance for oxygen in the titanite and the H_4SiO_4 added to the products (similar to the procedure of Carmichael, 1969).

The final titanite-free reaction, calculated as described, is as follows:

$$1.00Bi + 3.01H_2O + 1.18H^+ + 0.10Mg^{2+} + 0.16Fe^{2+} + 0.01Mn^{2+} = 0.58Chl + 1.14H_4SiO_4 + 0.18Ti^{4+} + 0.95K^+ + 0.01Na^+$$

(As in Ferry, 1979, there is a slight charge imbalance resulting from rounding errors.)

Generalized reactions (ignoring electrostatic charges) for mechanisms 1 and 2 are as follows (M = □ + Mg + Fe + Al^{VI} + Ti + Mn; T = Al^{IV} + Si; A = K + Na + □):

Mechanism 1

$$\underset{\text{Biotite}}{AM_3T_4O_{10}(OH)_2} + 3M + 3H_2O = \underset{\text{Chlorite}}{[M_3T_4O_{10}(OH)_2 + M_3(OH)_6]} + A$$

Mechanism 2

$$\underset{\text{Biotite}}{2AM_3T_4O_{10}(OH)_2} + 10H_2O = \underset{\text{Chlorite}}{1[M_3T_4O_{10}(OH)_2 + M_3(OH)_6]} + 4H_4TO_4 + 2A$$

For the reaction coefficients in Table 1, these generalized reactions were cast in terms of the observed biotite and chlorite compositions, using the relationships 1Bi = 1Chl for mechanism 1 and 1Bi = 1/2Chl for mechanism 2. The detailed reactions follow. In these reactions, K and Na are taken as monovalent; Mg, Fe, and Mn as divalent; Al as trivalent; and Ti and Si as quadrivalent.

Mechanism 1:

$$K_{0.95}Na_{0.01}\square_{0.23}Mg_{0.59}Fe_{1.65}Mn_{0.04}Ti_{0.18}Al_{1.63}Si_{2.72}O_{10}(OH)_2 + 6.04H_2O + 0.59Mg + 1.46Fe + 0.05Mn + 1.17Al = \square_{0.11}Mg_{1.18}Fe_{3.11}Mn_{0.09}Al_{2.80}Si_{2.71}O_{10}(OH)_8 + 0.01H_4SiO_4 + 0.18Ti + 6.03H^+ + 0.12\square + 0.95K + 0.01Na$$

Mechanism 2:

$$K_{0.95}Na_{0.01}\square_{0.23}Mg_{0.59}Fe_{1.65}Mn_{0.04}Ti_{0.18}Al_{1.63}Si_{2.72}O_{10}(OH)_2 + 2.55H^+ + 2.45H_2O = \square_{0.05}Mg_{0.59}Fe_{1.56}Mn_{0.04}Al_{1.40}Si_{1.36}O_5(OH)_4 + 1.36H_4SiO_4 + 0.18Ti + 0.18\square + 0.09Fe + 0.23Al + 0.95K + 0.01Na$$